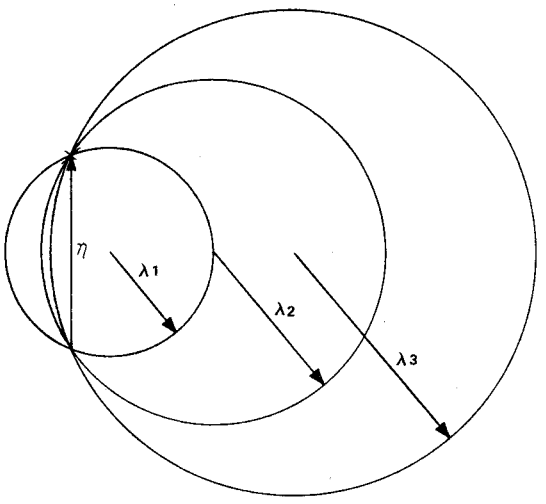

Fig. 2 Cone orientation for constant retro orientation.

desired half cone angle and the vehicle mass properties. A minimum half-cone angle was selected such that for a 2-sigma high-spin rate, 1.4 rev/sec, the total repointing capability was at least 10° greater than required.

The desired orientation of the induced cone is determined by the cone size and the desired repointing angle. Figure 2 presents the orientation of three cones at three different spin rates for the same orientation in space of the retro impulse. It can be seen that the roll orientation of the pitch motor impulse must be varied as a function of the spin rate to retain the desired retro orientation. The position on the cone of the retro maneuver can be expressed as

$$\cos\beta_R = (\cos\eta - \cos^2\lambda)/\sin^2\lambda \tag{4}$$

To properly orient the lateral retro maneuver and control the timing of the pitch and retro motor ignition, it is necessary to have onboard knowledge of the vehicle instantaneous roll attitude and spin rate. For the ATHENA mission, magnetometers were selected to provide the required data. The technique selected utilizes the knowledge of the earth's magnetic field and the nominal vehicle attitude just prior to velocity package respin to select an optimum orientation for the two magnetometers. The primary magnetometer is oriented normal to the vehicle spin axis at an angle such that the belly-down final pointing orientation results in a near zero magnetic field strength. As the vehicle spins, the magnetic field strength describes a sinusoidal variation.

This magnetic field strength will be achieved twice during each vehicle revolution. This belly-up/belly-down ambiguity is solved by installing a second magnetometer normal to the spin axis and 90° ahead of the primary magnetometer. By comparing the magnitude of the readings of the two magnetometers and the time between zero field strength readings, orientation and the spin period are determined. These data are then used in an onboard timing algorithm to determine the desired times of pitch motor and retro motor ignition based on the actual spin period and referenced to the time at which the vehicle is in a belly-down orientation.

Timing Algorithm

The retro timing algorithm is used to determine the time delay from belly-down to pitch motor ignition in order to control the cone orientation, and the time delay between pitch motor and retro motor ignition to be able to control the retro repointing angle as a function of the initial spin rate. Considering impulsive maneuvers, the time delay between pitch motor and retro motor ignition for any spin rate can be expressed as

$$\Delta t_R = \beta_R \dot{\beta} = I_T \cos\lambda \cos^{-1}[(\cos\eta - \cos^2\lambda)/\sin^2\lambda]/I_x p_0 \tag{5}$$

The desired roll orientation of the shift in the angular momentum vector, or center of the induced cone, from vertical in the initial vehicle roll plane is

$$\cos\Phi_D = \sin(\beta_R/2)/\cos\lambda \tag{6}$$

The roll orientation from belly-down at which the pitch motor impulse should be applied can be expressed by

$$\Phi_p = 90° + \Phi_D \tag{7}$$

The time of pitch motor ignition from belly-down is then

$$\Delta t_p = \Phi_p/p_0 \tag{8}$$

Onboard solution of these timing equations would require extensive onboard computational capability. To reduce cost and weight, an alternative approach was chosen based on a Chebyshev curve fit of the solution of the equations. Constants were entered into a timing function generator based on six-degree-of-freedom trajectory simulations at a series of spin rates over the expected range and the following equations:

$$\Delta t_R = A_R + B_R/SP \tag{9}$$

$$\Delta t_p = A_R + B_R SP \tag{10}$$

During vehicle preparation clips are placed on a matrix board. This matrix board consists of a number of circuit terminals and dummy terminals. The completed and open circuits then represent the four constants A_p, B_p, A_R, and B_R in a scaled, binary form. After despin to the nominal payload separation spin rate of 1 rev/sec and payload separation, the magnetometer data is examined to determine the actual spin period. Based on the preloaded constants and the measured spin period, the times Δt_p and Δt_R are calculated and stored in a timer. This timer is initiated when the magnetometers indicate that the belly-down attitude has been reached.

The lateral retro system described has flown on a number of operational flights on the ATHENA and successfully demonstrated its ability to control the radar linear and angular separation between the re-entry vehicles and the spent terminal stage.

Mach and Reynolds Number Effects on Turbulent Skin Friction Reduction by Injection

D. M. Bushnell,* R. D. Watson,† and B. B. Holley‡
NASA Langley Research Center, Hampton, Va.

Nomenclature

C_f = local skin friction coefficient
$C_{f,o}$ = no-blowing skin friction coefficient
F = wall blowing parameter $= \rho_w v_w/\rho_e u_e$
k = mixing length slope at wall

Received March 20, 1975; revision received May 8, 1975.
Index category: Boundary Layer and Convective Heat Transfer—Turbulent.

*Head, Fluid Mechanics Branch, High-Speed Aerodynamics Division.
†Aerospace Engineer, Applied Fluid Mechanics Section, High-Speed Aerodynamics Division. Member AIAA.
‡Mathematician, Applied Fluid Mechanics Section, High-Speed Aerodynamics Division.

$(\ell/\delta)_m$ = maximum mixing length/boundary-layer thickness
M = freestream Mach number
Re = Reynolds number
T = temperature
u,v = velocities in x and y directions
x,y = coordinates along and normal to surface respectively
δ = boundary-layer thickness
δ^+ = $\delta U_\tau/\nu_w$ where $U_\tau = (\tau/\rho_w)^{1/2}$, τ = maximum shear in the boundary layer, ν_w = kinematic viscosity
θ = momentum thickness
ρ = density

Subscripts

e = edge value
t = total value
w = wall value
x = based on x-coordinate
θ = based on θ

Introduction

THE conventional method of representing the influence of porous wall injection upon skin friction is on a plot of $C_f/C_{f,o}$ vs $2F/C_{f,o}$. An exhaustive review article by Jeromin[1] presents the available data in these coordinates (see Fig. 1 of Ref. 1). Jeromin's plot indicates a strong Mach number effect upon skin friction reduction due to blowing: for example, at $2F/C_{f,o}=2$, $C_f/C_{f,o}$ varies from $\simeq 0.1$ at $M\simeq 0$ to 0.7 at $M\simeq 6$. Several predictors[2-4] have examined the question of a Mach number effect in these coordinates since the publication of Jeromin's review. Reeves[2] calculates a weak Mach number effect, but his results indicate separate influences of Reynolds number and wall-to-total temperature ratio which could account for some of the apparent Mach number effect. Squire's[3] calculations (Fig. 28 of Ref. 3), employing a conventional mean field turbulence modeling procedure, indicate very little influence of either Reynolds number, Mach number, or T_w/T_t, at least for $Re_\theta > 8{,}000$ (the lower limit of his calculations). This result is similar to conclusions reached in the early work of Rubesin.[5] Landis[4] attributes Jeromin's Mach number effect to the influence of T_w/T_t.

The purpose of the present Note is to re-examine the question of possible Mach number influence on skin friction reduction caused by injection. The data which are most critical for resolving this question are those of Danberg.[6,7] These data comprise the only extensive, basic (two-dimensional) data set for turbulent flow with blowing above $M\simeq 3.5$. As will be shown, the preponderance of $M=0$ results

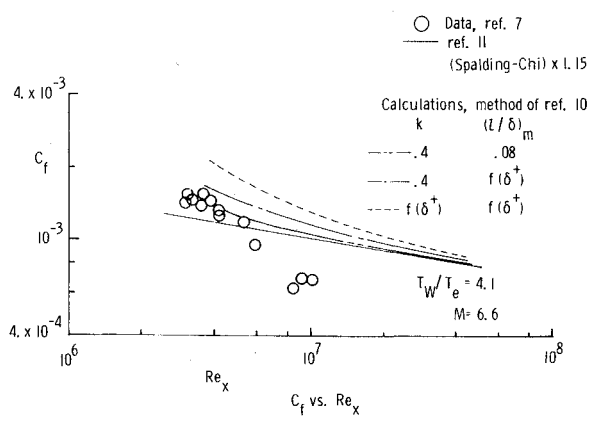

Fig. 1 Skin friction distributions for Danberg no-blowing case.

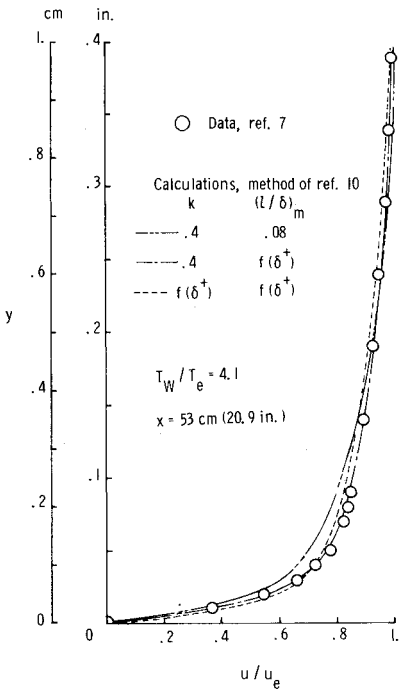

Fig. 2 Velocity profile comparison, tunnel stagnation pressure = 15.2 atm.

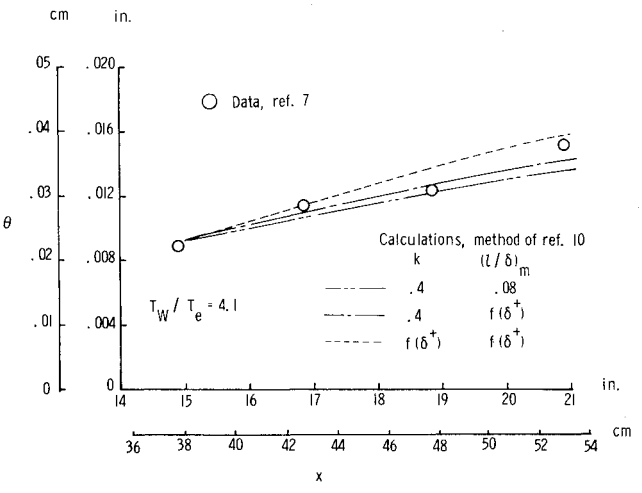

Fig. 3 Momentum thickness comparison, tunnel stagnation pressure = 15.2 atm.

now available agree with the $M\simeq 3$ data[5,8,9] and with the calculations of Rubesin[5] and Squire,[3] i.e., no strong Mach number influence is apparent, at least up to $M\simeq 3$. The Danberg[6,7] data will therefore be examined to ascertain whether the "Mach number independence" of $C_f/C_{f,o}$ vs $2F/C_{f,o}$ holds into the $M\sim 6.6$ range.

Since such a representation is sensitive to the $C_{f,o}$ value, a "zero blowing" case of Danberg[7] (runs 1-4, $T_w/T_e=4.1$, $M=6.6$) will be examined. $C_{f,o}$ calculations for this case using the method of Ref. 10 are shown in Fig. 1. The C_f "data" were obtained using velocity profile wall slopes.[7] Also shown is the Spalding-Chi prediction[11] increased by 15% which, as shown in Ref. 12, agrees with Mach 6 C_f data at high Reynolds numbers. Three numerical calculations are shown, all starting with the measured profile at the most forward "x-station," but with different methods of accounting for "low Reynolds number" effects.[13] The basic calculation employed low Reynolds number "amplifications"[13] of either k or $(\ell/\delta)_m$, or both. The low Reynolds number increase for $(\ell/\delta)_m$ (using δ^+ as a scaling function) was recently recon-

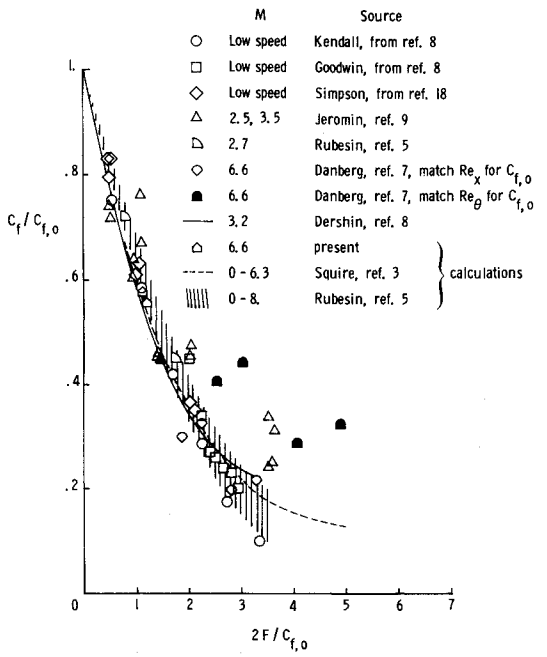

Fig. 4 Influence of surface injection on skin friction. $0 \leq M \leq 6.6$.

firmed in Ref. 14. Obviously the experimental "data" on Fig. 1 are not accurate at the higher Reynolds numbers.

The selection of which $C_{f,o}$ to use (which of the three calculations shown is more correct) was made on the basis of the momentum thickness and profile comparisons shown on Figs. 2 and 3. These comparisons clearly indicate that the calculation with fixed turbulence constants gives a velocity profile which is not full enough and too thin. Using a low Reynolds number amplification on both k and $(\ell/\delta)_m$ produces a profile which is too thick. The best of the present solutions appears to be the case where the turbulent shear in the outer region is increased by a low Reynolds number influence.[13,14] This is in agreement with Ref. 15, where the k value was found to be essentially invariant with Reynolds number for incompressible flow.

Therefore, based on the favorable profile and momentum thickness predictions, the $k=0.4$, $(\ell/\delta)_m = f(\delta^+)$ calculation results, shown on Fig. 1, can be used with some confidence as the appropriate $C_{f,o}$ for this Danberg case. When this is done (Fig. 4), the data for high blowing exhibit less scatter than in Ref. 1. It should be noted that Danberg's C_f "data" for high blowing should be more accurate than the zero or low blowing results, due to the thicker sublayers. When comparing blowing and no blowing C_f values, one has the option of making such comparisons at the same Re_x (same body station), or the same Re_θ (different body stations), a choice which is particularly important at low Reynolds number. Figure 4 indicates that when the same Re_x is used as a comparison, and the "correct" $C_{f,o}$ is employed, the Danberg data at $M \simeq 6.6$ agree with a substantial body of data and theory for Mach number 0-3.5. The obvious conclusion from Fig. 4 is that both data and theory indicate a negligible influence of Mach number upon nondimensional C_f reduction due to blowing, even when low Reynolds number effects are considered. Also shown on Fig. 4 is a prediction (using the method of Ref. 10) for the Danberg case with small blowing where low Reynolds number effects are most important (and hence were included in the calculation in the outer region). For this blowing case the suggestion of Baker and Launder[16] that δ^+ should be based upon maximum shear was utilized. It should be noted that the thicker boundary layers associated with blowing give higher δ^+ values, and hence decrease the "low Reynolds number" amplification rates when compared to the zero injection case, i.e., the low and no-injection cases have the maximum low Reynolds number influence.

In conclusion, the results of the present Note indicate that the Danberg $C_{f,o}$ data[7] are in error. When the influence of low Reynolds number amplification in the outer region of the boundary layer are included in a calculation method, accurate profiles and C_f values are obtained. When these $C_{f,o}$ values are used (at the same Re_x) to normalize the Danberg data with blowing, the available blowing data and the results of several calculation procedures agree and indicate negligible effect of Mach number on nondimensional C_f reduction due to blowing (for two-dimensional configurations, $0<M<6.6$). Also, the present calculations indicate that the low Reynolds number amplification on k, observed in Ref. 17, may not be correct.

References

[1] Jeromin, L. O. F., "The Status of Research in Turbulent Boundary Layers With Fluid Injection," *Progress in Aeronautical Sciences,* Vol. 10, pp. 65-189, edited by D. Kuchemann, 1970, Pergamon Press, London.

[2] Reeves, B. L., "A Two-Layer Model of High Speed Two- and Three-Dimensional Turbulent Boundary Layers With Pressure Gradient and Surface Mass Injection," Tech. Rept., SAMSO-TR-72-25, Nov. 1971, Space and Missiles Systems Organization, U.S. Air Force.

[3] Squire, L. C. and Verma, V. K., "The Calculation of Compressible Turbulent Boundary Layers With Fluid Injection," C. P. No. 1265, 1973, Aeronautical Research Council, London,

[4] Landis, R. B., "The Prediction of Compressible Turbulent Boundary-Layer Flows With Mass Addition," presented at the ASME Heat Transfer Conference, ASME Paper 72-HT-58, Denver, Colo., Aug. 1972.

[5] Rubesin, M. W., "The Influence of Surface Injection on Heat Transfer and Skin Friction Associated With the High-Speed Turbulent Boundary Layer," RM A55L13, Feb. 1956, NACA.

[6] Danberg, J. E., "Characteristics of the Turbulent Boundary Layer With Heat and Mass Transfer at $M=6.7$," Naval Ordnance Lab., White Oak, Silver Spring, Md., TR 64-99, Oct. 1964.

[7] Danberg, J. E., "Characteristics of the Turbulent Boundary Layer With Heat and Mass Transfer: Data Tabulation" NOL TR 67-6, Jan. 1967, Naval Ordnance Lab., White Oak, Silver Spring, Md.

[8] Dershin, H., Leonard, C. A., and Gallaher, W. H., "Direct Measurement of Skin Friction on a Porous Flat Plate With Mass Injection," *AIAA Journal,* Vol. 5, Nov. 1967, pp. 1934-1939.

[9] Jeromin, L. O. F., "An Experimental Investigation of the Compressible Turbulent Boundary Layer With Air Injection," ARC 28 549, Nov. 1966, Aeronautical Research Council, Ministry of Aviation, London.

[10] Bushnell, D. M. and Beckwith, I. E., "Calculation of Nonequilibrium Hypersonic Turbulent Boundary Layers and Comparisons with Experimental Data," *AIAA Journal,* Vol. 8, Aug. 1970, pp. 1462-1469.

[11] Spalding, D. B. and Chi, S. W., "The Drag of a Compressible Turbulent Boundary Layer on a Smooth Flat Plate With and Without Heat Transfer," *Journal of Fluid Mechanics,* Vol. 18, Jan. 1964, pp. 117-143.

[12] Cary, A. M., Jr. and Bertram, M. H., "Engineering Prediction of Turbulent Skin Friction and Heat Transfer in High-Speed Flow," TN D-7507, July 1974, NASA.

[13] Bushnell, D. M. and Alston, D. W., "Calculation of Transitional Boundary-Layer Flows," *AIAA Journal,* Vol. 11, April 1973, pp. 554-556.

[14] Bushnell, D. M., Cary, A. M., Jr., and Holley, B. B., "Mixing Length in Low Reynolds Number Compressible Turbulent Boundary Layers," *AIAA Journal,* Vol. 13, Aug. 1975, pp. 1119-1121.

[15] Huffman, G. D. and Bradshaw, P., "A Note on von Karman's Constant in Low Reynolds Number Turbulent Flows," *Journal of Fluid Mechanics,* Vol. 53, Part 1, 1972, pp. 45-60.

[16] Baker, R. J. and Launder, B. E., "The Turbulent Boundary Layer With Foreign Gas Injection—I. Measurements in Zero Pressure Gradient," *International Journal of Heat Mass Transfer,* Vol. 17, pp. 275-291, Pergamon Press, 1974.

[17] Bushnell, D. M. and Morris, D. J., "Shear-Stress, Eddy-Viscosity, and Mixing-Length Distributions in Hypersonic Turbulent Boundary Layers," TM X-2310, Aug. 1971, NASA.

[18] Anderson, L. W. and Morse, H. L., "A Turbulent Model Study for the Multicomponent Nonsimilar Turbulent Boundary Layer Program," Tech. Rept. AFWL-TR-71-57, Oct. 1971.